Helium-3 Density Measurements Using Atomic Pressure Broadening

A thesis submitted in partial fulfillment of the requirement
for the degree of Bachelor of Science with Honors in Physics from
The College of William and Mary

by

Sara Elizabeth Mohon

Accepted for _____
(Honors)

_____
Gina Hoatson, Director

_____
Todd Averett, Advisor

_____
Seth Aubin

_____
Gunter Luepke

Williamsburg, VA
April 28, 2009

ABSTRACT

Helium-3 (^{3}He) gas is used as an effective neutron target at many particle accelerators studying the neutron spin structure. Its nucleus usually has two protons of opposite spin and one neutron determining the overall spin of the nucleus. Typically, the gas is polarized using optical pumping and spin exchange through the use of potassium (K) and rubidium (Rb). A density measurement of the ^{3}He within such a mixture of gases is important before accelerator experiments can begin. This paper describes how such a ^{3}He density measurement can be obtained through pressure broadening of K D2 absorption lines. This research shows the absorption lines were broadened by directing a Titanium Sapphire (Ti:Sapph) laser through a heated oven holding the ^{3}He gas mixture. The ^{3}He density of the neutron target named Fini at the College of William and Mary was measured to be 7.12 +/- 0.83 amg due to fitting errors. Experimental error could be minimized in the future with an automated frequency tuner, more absorption measurements per wavelength, and a focusing lens in front of each photodiode.

CONTENTS

INTRODUCTION

Many scientists are curious about the spin structure of neutrons. To probe their inner structure, a high energy particle accelerator is needed such as the one at Thomas Jefferson National Accelerator Facility (TJNAF). This particle accelerator shoots electrons at any desired target. Neutron targets however are not easy to create. They have very short half-lives of about ten minutes on their own. In order to have a neutron target that will not disappear during an experiment, a different substance must be used. This is why most laboratory sites use glass targets filled with ^{3}He gas to serve as an effective neutron target. A ^{3}He nucleus has two protons and one neutron as shown in Figure 1. About ninety percent of the time, a ^{3}He nucleus will be in the state that has the two protons in opposite spins so that the overall spin of the nucleus is determined by the spin of the neutron [1].

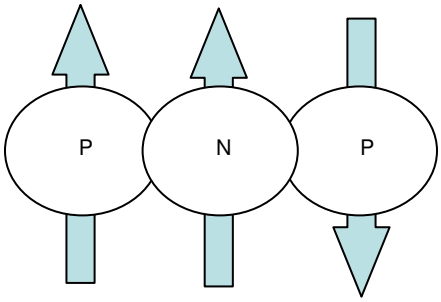

Figure 1: Drawing of ^{3}He nucleus

Is there an alternative to ^{3}He? Yes, deuterium (^{2}H) is an alternative material but it has a drawback concerning polarization. Its nucleus, the deuteron, has one proton and one neutron. This nuclear set-up is actually more favorable than ^{3}He because there is a one in two chance instead of a one in three chance of hitting the neutron with an electron. However, there is no way to polarize ^{2}H while it is in the gaseous form because it is diatomic. Polarization-related effects from scattering from the two protons in a ^{3}He sample largely cancel, leaving the neutron as the focus of polarization procedures [2].

A typical ^{3}He target cell is shown in Figure 2. These are glass cells that are hand-blown at Princeton University by a skilled professional. Once they are produced, the pieces are sent to either the College of William and Mary or the University of Virginia so that it can be assembled and filled with nitrogen (N_2), potassium (K), rubidium (Rb), and ^{3}He. At these locations, the cells are attached to a vacuum system before being carefully filled [3]. Once filled, the cell is then ready to be polarized and characterized.

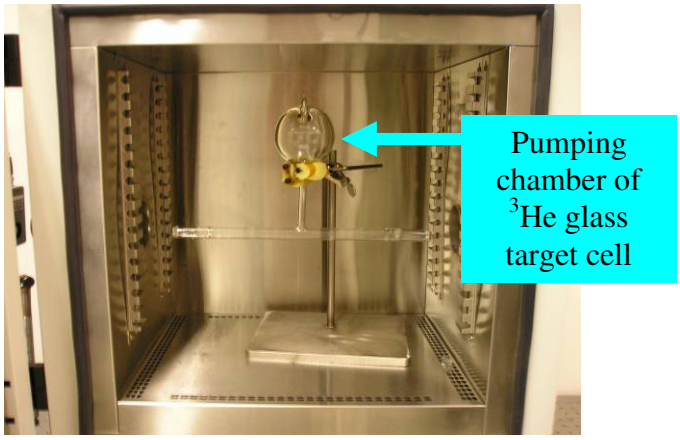

Figure 2: Typical ^{3}He target cell suspended in an oven

Scientists try to control and measure the properties of target material in their experiments as much as possible. This is why the target goes through multiple tests and preparation before the large particle accelerator experiment. Some of these preparations include glass wall thickness measurements, ^{3}He density measurements, and polarization of ^{3}He nuclei [1]. The purpose of this paper is to describe the preparation and procedure to measure the density of ^{3}He target cells using a Titanium Sapphire (Ti:Sapph) laser.

As mentioned above, the neutron's spin in a ^{3}He atom is mostly responsible for the nucleus' overall spin. Since this spin can be parallel or anti-parallel to an external field, physicists use lasers and magnets to polarize the ^{3}He nuclei as much as possible so

that most will have the same spin direction. The higher the ^{3}He polarization, the more useful the cell is in an accelerator experiment [3].

Polarization of ^{3}He nuclei occurs through processes called optical pumping and spin exchange. Optical pumping occurs first by heating the cell in an oven at 230˚C in order to vaporize the Rb and K. The Rb vapor is then polarized using a diode laser with a circularly polarized beam. Within an applied external field of 13 G, the Rb and K vapor exhibits Zeeman splitting [2].

Polarization is transferred from the Rb to the K and from there to the ^{3}He nucleus during collisions. The ^{3}He becomes polarized through the process called spin exchange. Spin exchange is the hyperfine-like interaction of ^{3}He nuclei and K atoms whereby the spin of the polarized K atom is transferred to the ^{3}He nucleus during collisions [3]. Once the K atom has lost its polarization, it is immediately pumped back into its polarized state with the diode laser and Rb. The addition of K to the target cell is meant to polarize ^{3}He more efficiently [4].

The atomic transitions, due to the Zeeman Effect actually split further due to the polarized ^{3}He surrounding the Rb and K vapor. The shift due solely to the ^{3}He is directly proportional to the polarization of the ^{3}He within the target cell. In order to determine the amount of shift due to the ^{3}He, the polarization direction of ^{3}He is reversed and the shift is again measured. The difference between these two states gives the shift in atomic transitions due to the polarized ^{3}He [5].

MATERIALS AND METHODS

OVERVIEW

For this experiment, a Ti:Sapph laser, a Verdi pump laser, a computer, an oven, and an appropriate optical setup is necessary to measure the density of a ^{3}He target cell. The Verdi laser is used to pump the Ti:Sapph laser while the output of the Ti:Sapph laser enters the oven that contains the target cell and exits through the other side. Heating of the target cell and multiple density measurements will give an analysis of how temperature and density are related. Photodiodes will be placed before and after the oven glass windows in order to measure the relative intensity of the laser light that is transmitted through the cell over a range of frequencies provided by the frequency scanning capability of the Ti:Sapph laser. Around 766.5 nm at 125 °C there will be a large absorption peak corresponding to the potassium D2 absorption line. The width of this absorption line is larger at higher densities. This broadening of the K absorption is called pressure broadening and is what we use to determine the ^{3}He density of the target cell [6]. A schematic of the necessary experimental setup is shown in Figure 3, with the laser path shown in blue. A picture of the lasers and the wavemeter are shown in Figure 4.

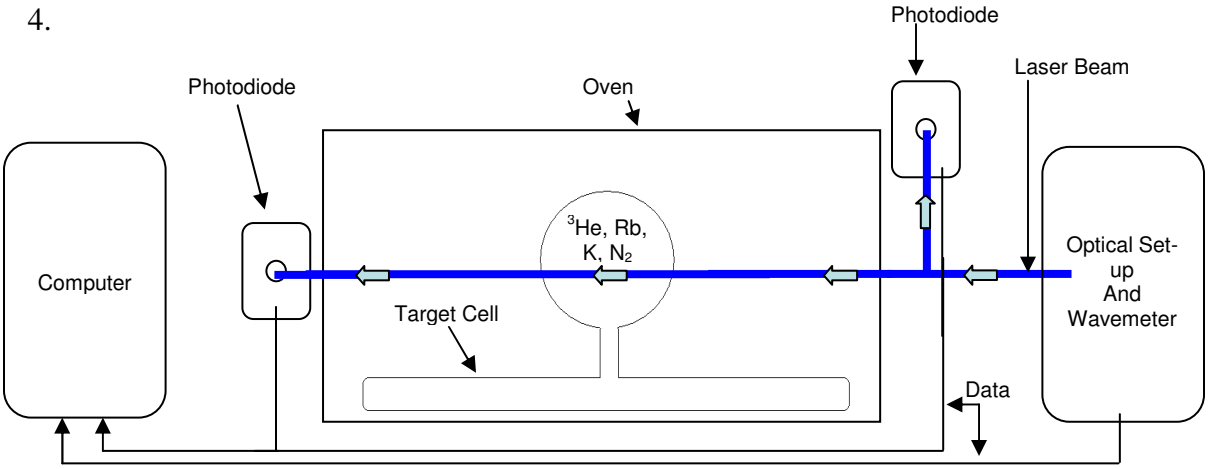

Figure 3: Schematic of experimental setup

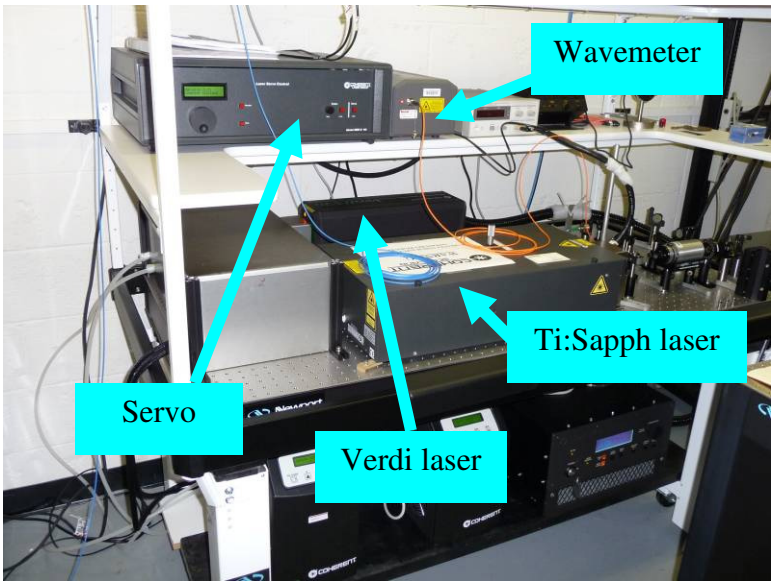

Figure 4: Ti:Sapph optics table.

TI:SAPPH OPTICS TABLE

On the Ti:Sapph optics table there is the Servo, the Verdi pumping laser, Ti:Sapph laser, and two light paths for the wavemeter fiber and the Ti:Sapph laser fiber as shown in Figures 4 and 5. Once laser light is emitted from the Ti:Sapph box, the light passes through a filter to remove any remaining Verdi light and then enters a polarizer. This polarizer adjusts how much light will be allowed to enter both the wavemeter fiber and the Ti:Sapph laser fiber later on. It is important to monitor this closely because if too much power enters the wavemeter through the wavemeter fiber, then the wavemeter can be damaged. For this specific experiment, a Bristol wavemeter was used and 30mW was not exceeded. Next, Figure 5 shows that the beam approaches the isolator. The purpose of the isolator is to eliminate reflected laser light into the Ti:Sapph cavity. At the front of the isolator is a beam splitter which allows us to create a second beam path for the wavemeter fiber. This path is shown by the red line in Figure 5. The light is coupled to the wavemeter fiber and fed to the wavemeter itself. The remaining light path that passes

through the isolator, is guided to another fiber coupler to be used in the pressure broadening experiment inside the oven. This Ti:Sapph laser path is shown in Figure 5 in blue.

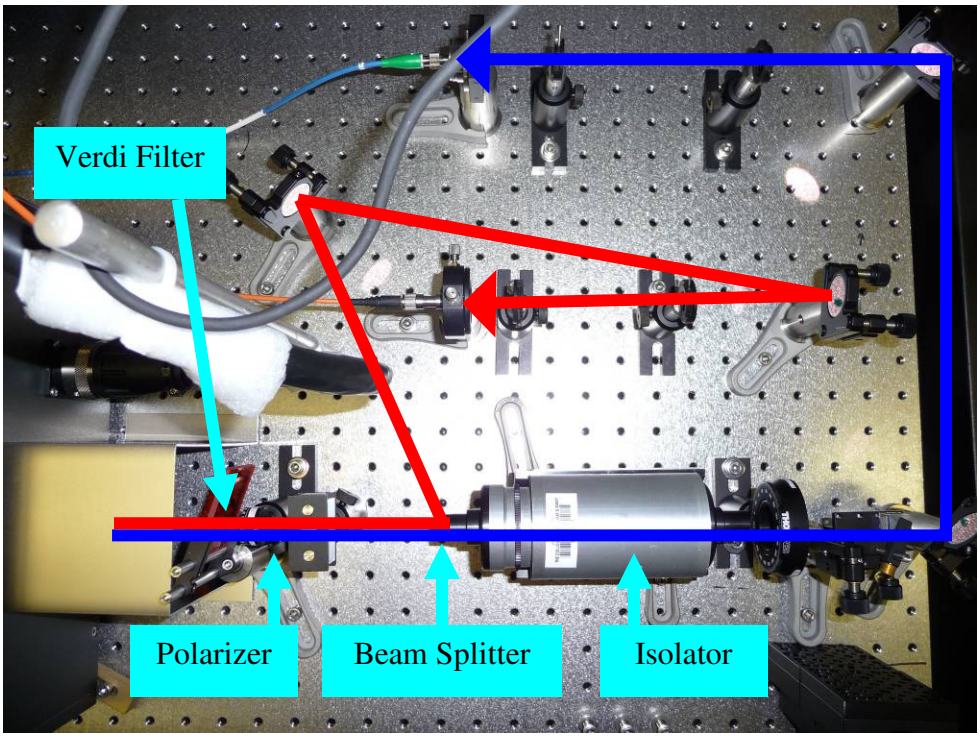

Figure 5: Wavemeter laser path in red and Ti:Sapph experiment laser path in blue.

OVEN OPTICS TABLE

On the oven optics table sits the oven, optics to guide the Ti:Sapph laser light into the oven, the two photodiodes, the data acquisition (DAQ) device and the oven thermocouples as shown in Figure 6. When laser light from the Ti:Sapph laser fiber enters the oven optics table, it reaches another fiber coupler and then hits a beam splitter. This beam splitter allows for the reference photodiode above the beam splitter to measure the relative intensity of laser light about to enter the oven. The other laser path is guided by mirrors into the oven to penetrate the pumping chamber of the target cell inside. Once penetrated, the remaining laser light exits through the other side of the oven to be

measured by the other photodiode, named the absorption photodiode. A ratio of absorbed intensity over reference intensity will produce the absorption plot versus wavelength as wanted.

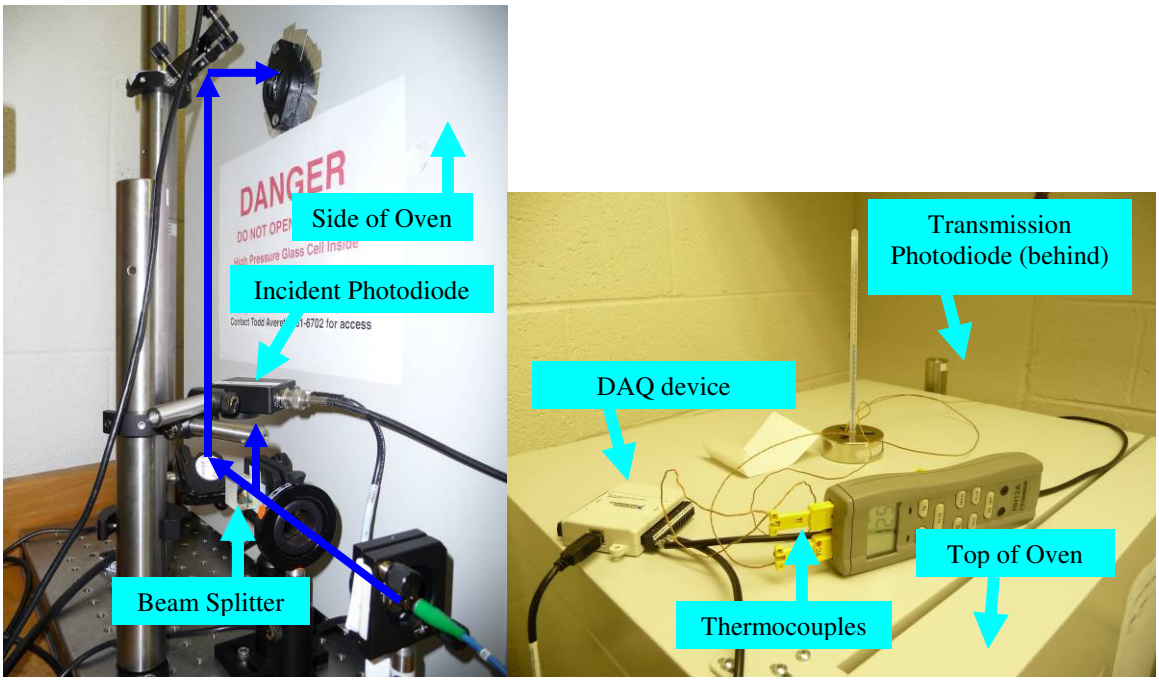

Figure 6: Side and top views of oven optics table. Path of laser light shown in dark blue line.

It is also worth mentioning that inside the oven, thermocouples are used to monitor temperature stability of the cell's pumping chamber and the oven. A uniform and steady temperature inside the oven is necessary to collect good, clean data. Fluctuation in temperature can cause erratic jumps of the absorption versus wavelength plot. An example of this erratic behavior is shown in Figure 7.

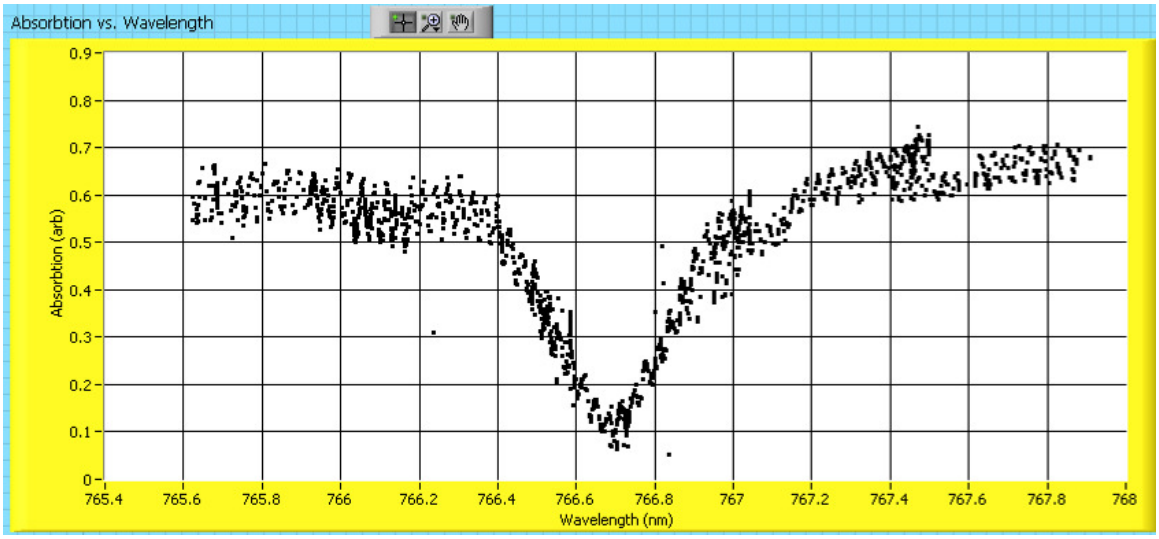

Figure 7: Erratic jumping can occur when the mode in laser is changed when tuning the frequency. This can change the output power and polarization of the laser light and produce erratic jumps in data. A possible example of this mode jumping is shown above from 767- 767.5 nm. From 766-766.2 nm a possible fluctuation in oven temperature is present.

DATA ACQUISITION

LabVIEW code will read voltage produced by the photodiodes, the Ti:Sapph wavelength, and the Ti:Sapph power throughout the whole experiment. Wavemeter code and photodiode code have been integrated into one program called PressureBroadDaq.vi so various graphs relating wavelength, power, absorption, and photodiode voltage and can be achieved after pressing a start button and gathering data. Screen shots of the photodiode and wavemeter code are shown in Figure 8 and 9 respectively.

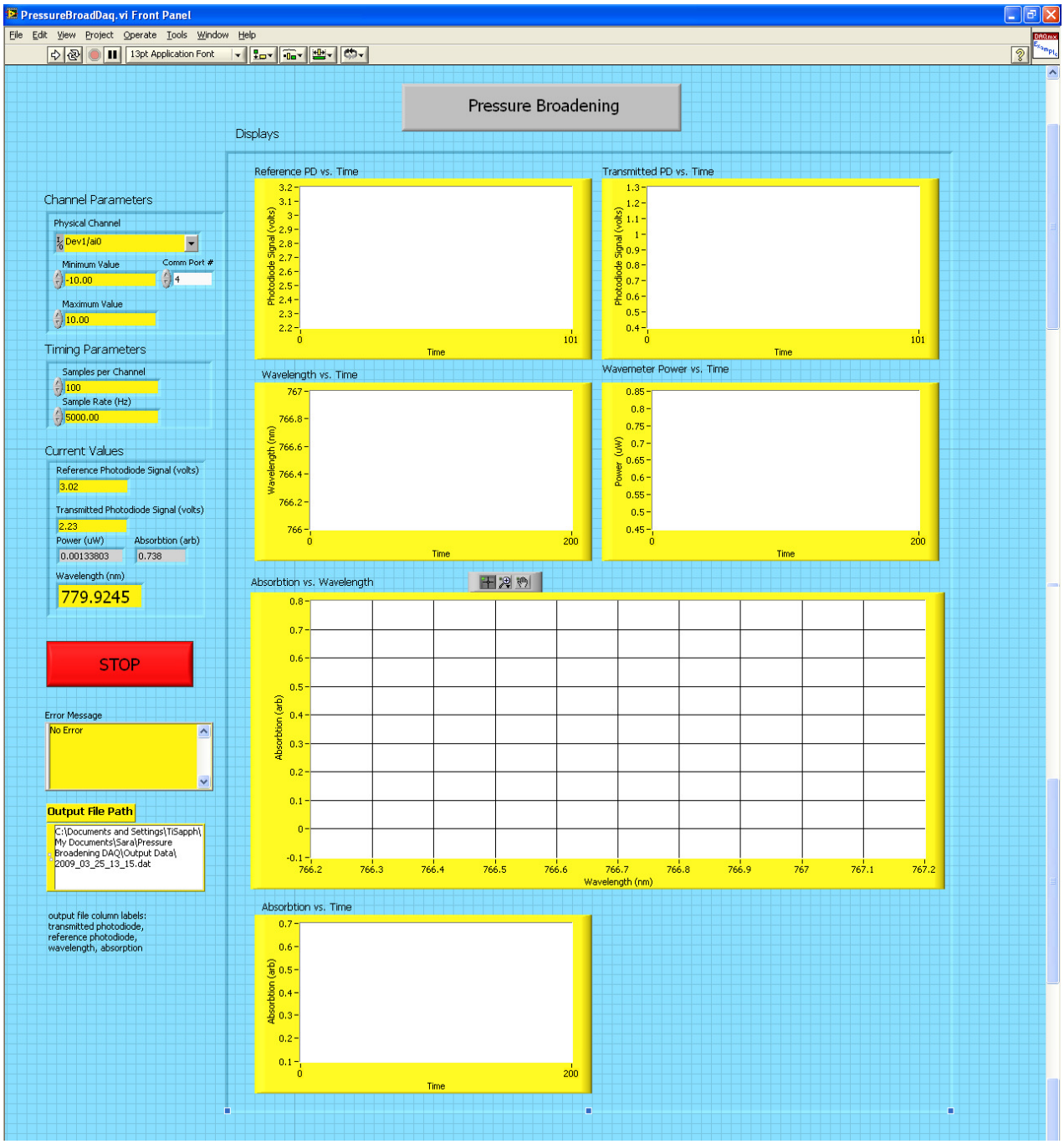

Figure 8: LabVIEW front panel screenshot of photodiode code. Absorption vs. wavelength plot is important for finding absorption.

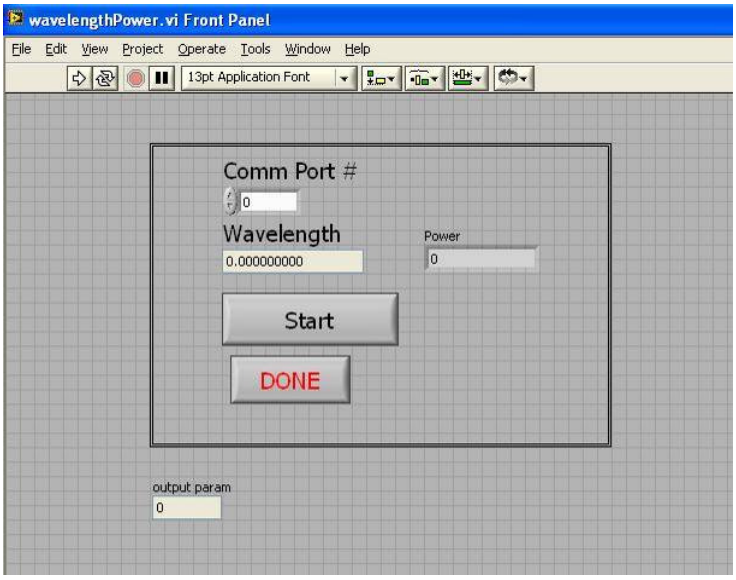

Figure 9: LabVIEW front panel screenshot of wavemeter code. Reads wavelength and power from wavemeter.

Specific graphs in the PressureBroadDaq.vi include photodiode voltage versus sample number. This is used to make sure that the voltage on the reference photodiode is larger than the voltage on the absorption photodiode. This VI also has graphs of wavelength versus time and wavemeter power versus time. These values are important to perform the correct wavelength scan and to not exceed the maximum wavemeter power. Lastly, this VI has a graph of absorption versus wavelength. This is the graph that should ideally look like Figure 10 which will be discussed shortly.

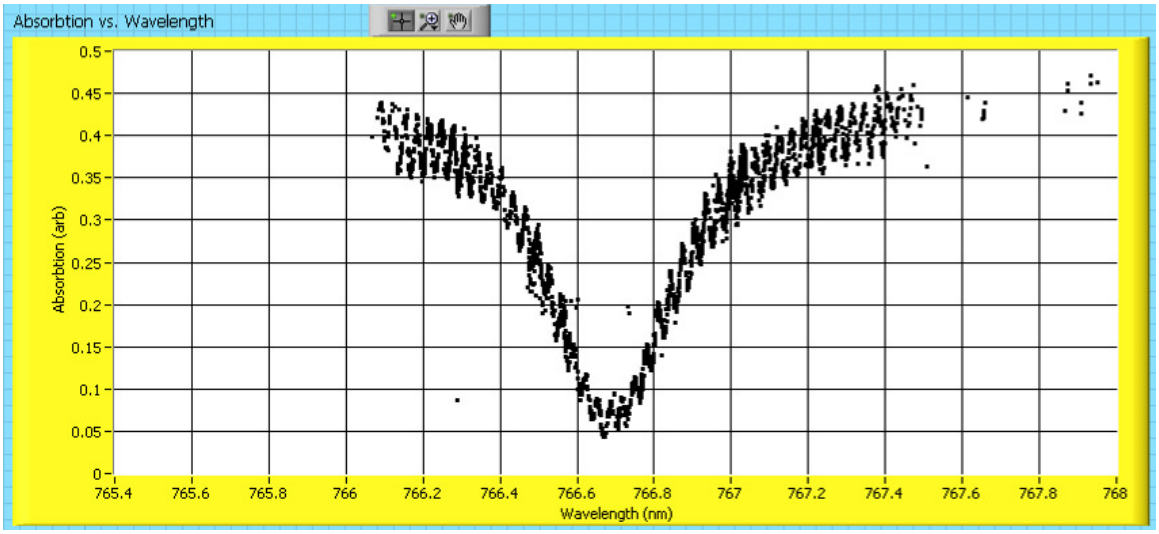

Figure 10: Ideal Absorption vs. wavelength plot.

The target cell will be placed inside the oven on an adjustable metal stand and then aligned so that the laser travels through the pumping chamber of the cell. If the laser beam does not travel straight through the pumping chamber, then the signal will not be detected at the second photodiode [3]. Typically some of the laser beam will reflect off the sides of the pumping chamber and bounce back and forth before reaching the second photodiode. These reflections can create a small interference signal called the etalon effect of which an example can be seen in Figure 11 [4]. If the laser beam is completely perpendicular with the front of the pumping chamber, then the etalon effect from this surface is minimized [2]. Much care was taken to achieve the largest signal possible from the second photodiode and minimize the etalon effect. The source or sources of the etalon in Figure 11 is unknown until correct curve-fitting is applied. The correct glass thickness of the source or sources can then be extracted from the curve-fitting and compared to the known glass thicknesses values of the target cell, oven windows, and the photodiode windows.

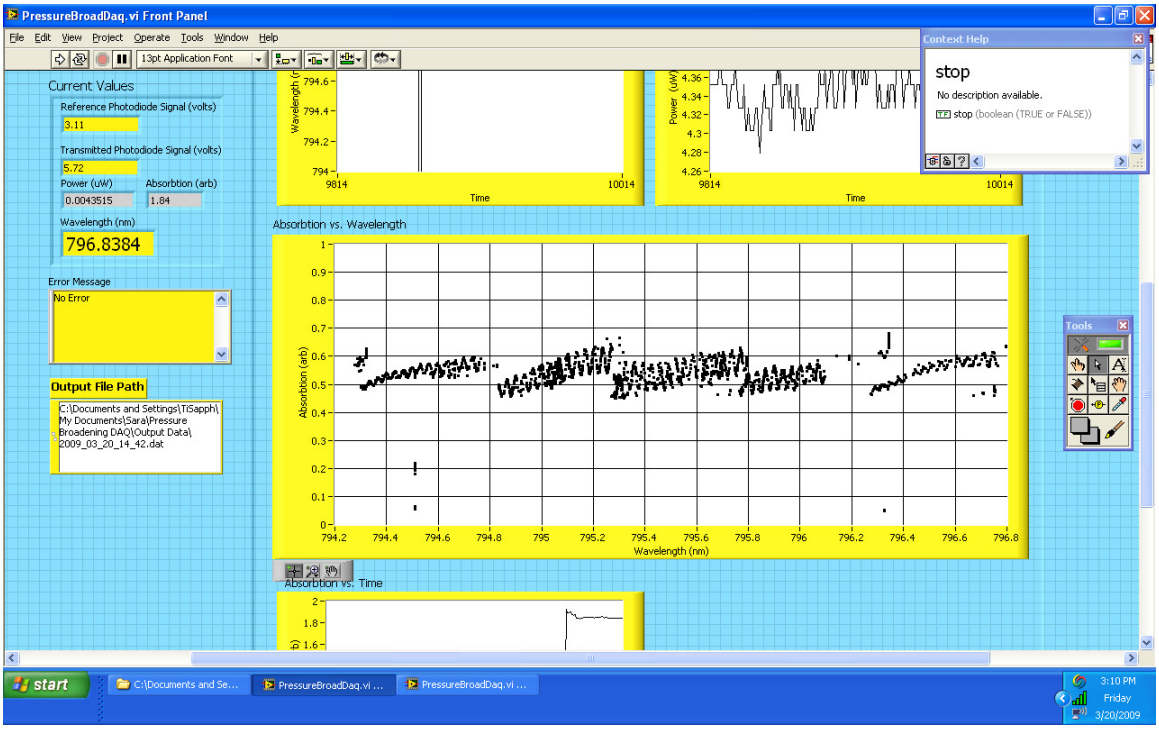

Figure 11: Pure etalon effect without any absorption. Etalon effect has characteristic sine wave.

The integration of the two codes has provided the ratio of the input intensity over the output intensity (I_{in}/I_{out} or absorption) versus the frequency of the laser [1]. Again, when the Ti:Sapph laser reaches 766.5 nm at 125°C, a large K absorption is detected. If the cell contained only pure K at low density, then the absorption signal for the D2 line would be at shifted to the left of 766.5 nm with minimal broadening [6]. The ^{3}He within the cell causes this absorption to have a broader linewidth centered at 766.5 nm. As the K and ^{3}He collide with each other, the energy of the K transition broadens. Therefore the width of the K absorption is related to the energy spread of the K transition. The linewidth of the K absorption is an indirect measurement of the ^{3}He density; the larger the linewidth, the larger the ^{3}He density [2].

PERFORMING A SCAN

Using the Ti:Sapph laser to obtain data to be displayed on the LabVIEW pressure broadening VI is not an automated process. The laser frequency changes by use of two knobs: a frequency coarse tuner and a frequency fine tuner. The coarse tuner is located on the top of the Ti:Sapph laser box itself while the fine tuner is located on the black Servo box on the shelf above the laser optics table. The fine tuner covers a maximum frequency range of about 0.4 nm which makes taking a larger scan more challenging especially since the coarse tuner moves at a minimum of 0.4 nm steps. These restrictions on the Ti:Sapph frequency tuning requires a practiced investigator to record data for a frequency range only once.

SAFETY

When aligning the cell with the laser, many safety precautions were taken. Safety is very important because the target cells are under significant pressure and have the possibility of exploding if mishandled. To avoid harm, handlers of the target cell wore long sleeves, gloves, foam earplugs, and a face shield. Special laser safety glasses that block light near the 800 nm range were worn whenever the laser beam was on. The light reflected from the Ti:Sapph laser can damage the retina before the human eye can blink [3]. A picture of this safety equipment is shown in Figure 12.

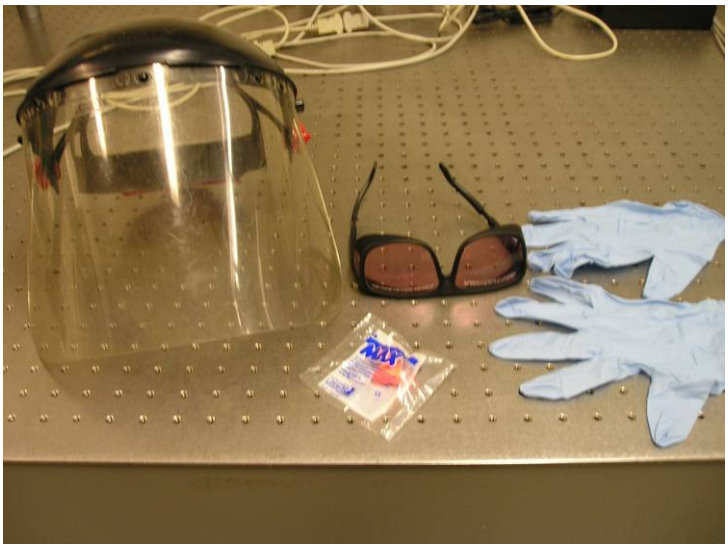

Figure 12: Safety equipment

After the Verdi pumping laser, a light box is situated to house the Verdi laser light produced. This light box shields all green laser light from entering the human eye as seen in Figure 13. The laser glasses used in the lab are only suitable for near infrared regions and not green regions, hence the need for the light box.

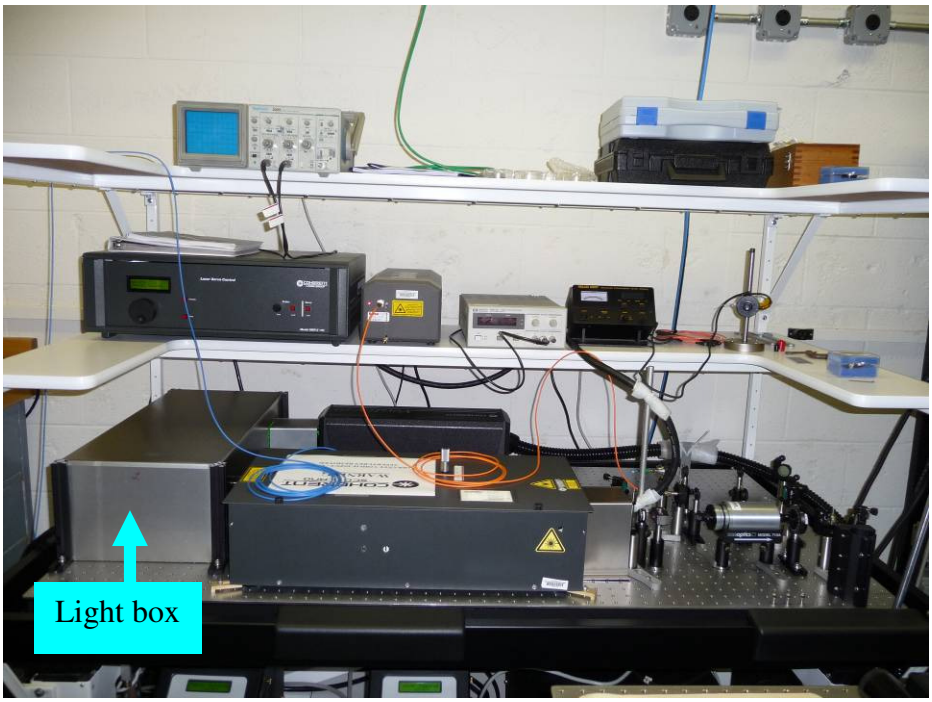

Figure 13: Verdi light box.

CURVE FITTING

After the cell is scanned, the K absorption plot will need to be analyzed using a curve fitting routine. At TJNAF, the program ROOT creates a Lorentzian curve fit for the data that minimizes chi squared (χ^2) [3]. The Lorentzian equation that ROOT uses is shown in Equation 1 where I_T is the intensity of transmitted light, I_0 is the intensity of incident light, A is the absorption amplitude, T_d is the collision duration, υ_c is the resonant frequency, gamma (γ) is the measured linewidth of the K D2 absorption line, and B is the offset. By this method, the value γ was divided by a conversion function in amagats or amg to determine the density of ^{3}He in the target cell [7]. An amagat is a unit of number density at STP [2]. More explicitly, 1 amagat = $2.6868 \cdot 10^{19}$ atoms cm^{-3} [5]. The conversion function that divides γ and gives the density of the cell is a measured quantity that is not precisely known. It is extracted from measuring the linewidth in GHz of the K absorption for various known densities of ^{3}He in a given volume [4]. The slope of the linewidth versus density will give a number near 21.3 amg for the K D2 absorption line [8].

$$(1) \qquad \ln(I_T/I_0) = \frac{A[1 + 0.6642*2\pi*T_d(\upsilon - \upsilon_c)]}{(\upsilon - \upsilon_c)^2 + (\gamma/2)^2} + B$$

Equation 1: Lorentzian equation used for curve fitting. I_T is the intensity of transmitted light, I_0 is the intensity of incident light, A is the absorption amplitude, T_d is the collision duration, υ_c is the resonant frequency, γ is the measured linewidth of the K D2 absorption line, and B is the offset.

While the ROOT system works well, it would be convenient and beneficial to have an in-house Lorentzian curve fitting routine for use in LabVIEW at the College of William and Mary. This is the final task to complete and much progress has been made. Please see the Results section for further explanation.

RESULTS

A scan of the target cell named Fini was conducted to determine preliminary parameters such as photodiode gain settings and oven temperature. At an oven temperature of 80°C and wavelength of near 766.5 nm, a sinusoidal signal was detected due to the unavoidable etalon effect. The periodic upward sloping frequencies were later attributed to mode changes within the laser. At higher temperatures, such as 125°C the absorption signal became more pronounced and much cleaner data was recorded. Figures 14, 15, and 16 show various laser power settings and the data they produced. Typically, a cell at a temperature of 125°C and laser power of 20mW into the blue fiber produced clean data.

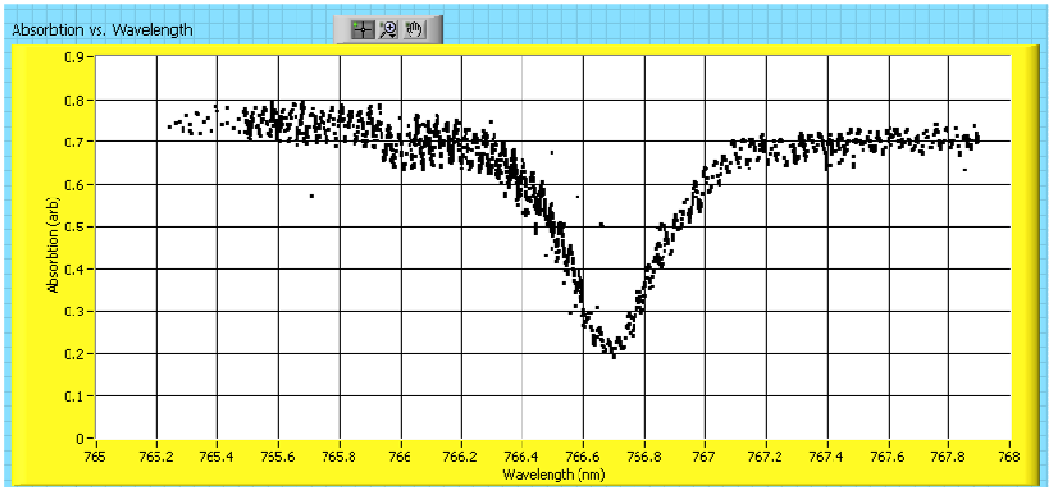

Figure 14: Absorption at temperature of 125°C and laser power of 15mW into the blue fiber.

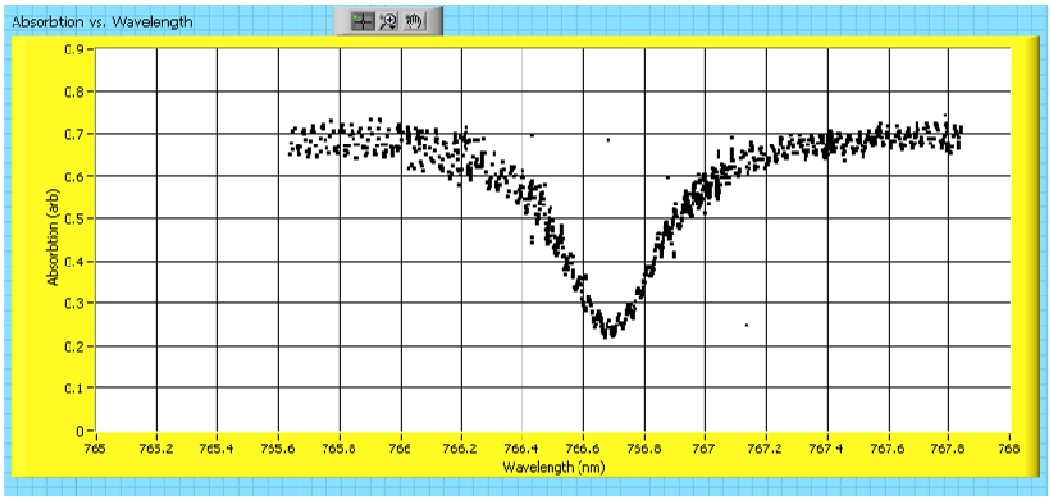

Figure 15: Absorption at temperature of 125°C and laser power of 20mW into the blue fiber.

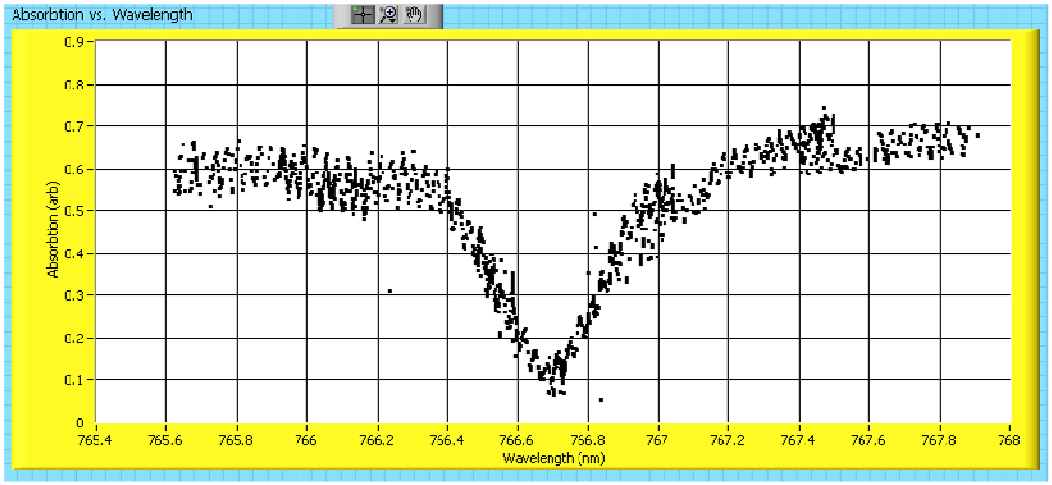

Figure 16: Absorption at temperature of 125°C and laser power of 25mW into the blue fiber.

While this paper is mainly concerned with the K D2 absorption line at 766.5 nm, there also exists several other absorption lines within the Ti:Sapph's frequency range. See Table 1 for the absorption list and respective characteristic wavelengths. Energy level diagrams for Rb and K are given in Figures 17 and 18 respectively [9, 10]. An absorption plot which includes all absorption lines can be seen in Figure 19. This shows that the potassium D2 absorption line is the largest absorption of all four which is to be expected because there is more K in the target cell than Rb. This is why we chose to determine the ^{3}He density using this absorption line and not the others.

Rubidium	D1	794.7 nm
	D2	780.0 nm
Potassium	D1	770.1 nm
	D2	766.5 nm

Table 1: Approximate absorption line locations at 125°C.

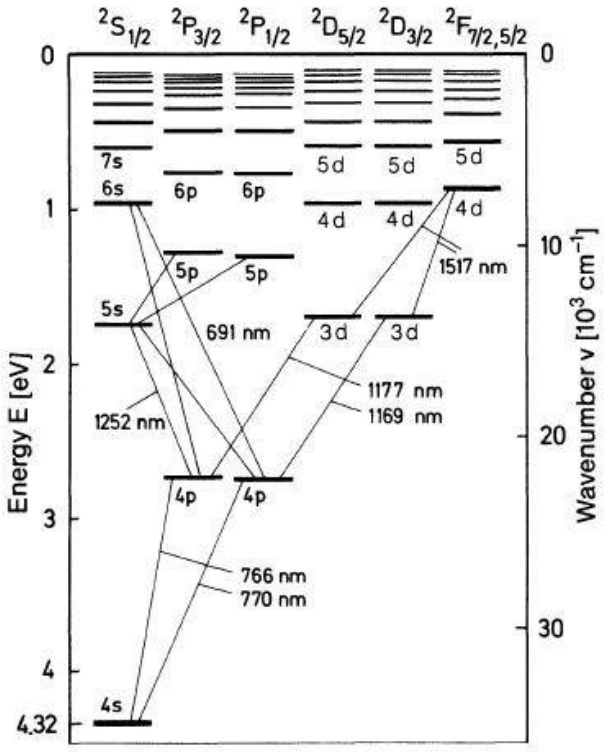

Figure 17: Energy Level diagram of K transitions.

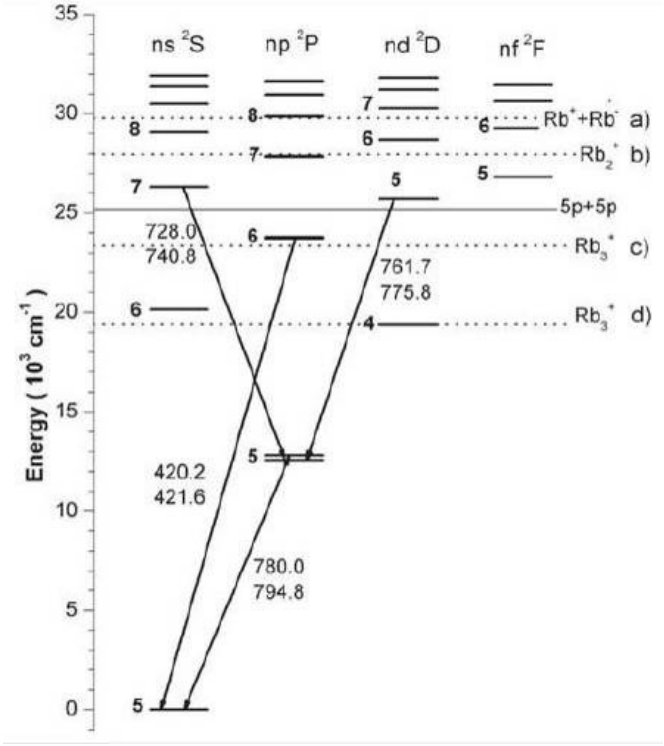

Figure 18: Energy Level diagram of Rb transitions.

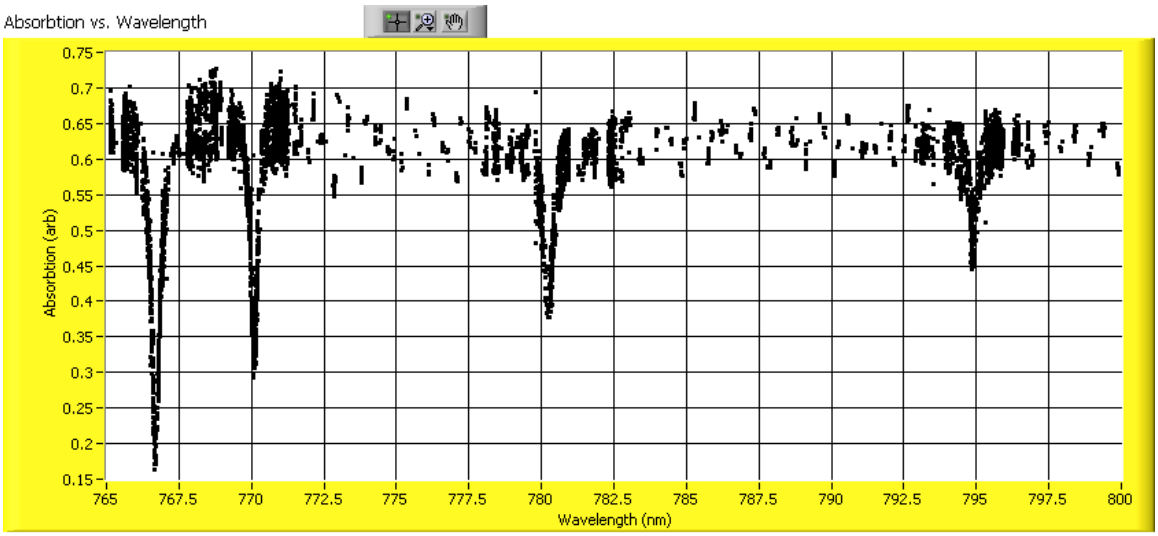

Figure 19: All absorption lines at 125°C.

The current curve-fitting code is operating but not ideal. Using a Levenberg-Marquardt (Lev-Mar) non-linear curve-fitting technique in LabVIEW, the absorption data can be very well fitted but without the etalon contribution. It has been a mystery as to

why the Lev-Mar VI does not recognize the sine function as a model equation to fit to. All curve fits in this paper will not include the sinusoidal term for this reason. All curve-fitting was completed using the lorentzian_no_etalon.vi file.

From Singh's paper [7] we know that the linewidth of the K D2 absorption line is proportional to the density of the buffer gas. His preliminary results for the conversion function of the K D2 absorption line is 21.3 amg at 398 K. We also know that there is much more K than N_2 within the target cell rendering the $[N_2]$ term negligible. This information can be summarized as shown in Equations 2, 3, and 4 [8]. ^{3}He densities for the target cell Fini were calculated using Equations 3 and 4 and are shown in Table 2. Averett's data shows that Fini was filled with 7.34 amg of ^{3}He [11].

(2) $\gamma = \langle\sigma\upsilon\rangle_{K\text{-}3He}[^3He] + \langle\sigma\upsilon\rangle_{K\text{-}N2}[N_2]$

(3) where conversion function $\langle\sigma\upsilon\rangle_{K\text{-}D2\text{-}3He} = (20.3 +/- 0.9)(T / 353\ K)^{0.42 +/- 0.31}$ in GHz/amg

(4) hence ^{3}He density $\approx [^3He] = \dfrac{\gamma}{(20.3 +/- 0.9)(T / 353\ K)^{0.42 +/- 0.31}}$.

Equations 2, 3, and 4: Density and conversion function equations using K D2 absorption line.

Target Cell Name	File Name	Line Absorption	Temp T (K)	Power into blue fiber (+/- 0.2 mW)	γ of Best Fit (GHz)	^{3}He Density (amg) Fitting uncertainty only
Fini	2009_03_25_14_25	K-D2	398	10.0	102.93 (+/- 9.05)	4.82 (+/- 0.42)
Fini*	2009_03_25_14_43	K-D2	398	15.0	157.73 (+/- 10.69)	7.38 (+/- 0.50)
Fini*	2009_03_25_15_07	K-D2	398	20.0	166.39 (+/- 23.18)	7.79 (+/- 1.08)
Fini	2009_03_25_15_24	K-D2	398	25.0	130.32 (+/- 15.89)	6.10 (+/- 0.74)
Fini*	2009_03_25_15_46	K-D2	398	5.0	145.30 (+/- 19.72)	6.80 (+/- 0.92)
Fini*	2009_04_01_13_49	K-D2	398	15.0	139.51 (+/- 17.94)	6.53 (+/- 0.84)
Fini	2009_04_01_14_44	K-D2	398	20.0	124.06 (+/- 17.20)	5.81 (+/- 0.80)

Table 2: Table of ^{3}He density calculations using K D2 line absorption. The rows with * did not have an intensity absorption ($I_{Transmitted}/I_{Incident}$) of less than 0.10.

The density measurements in Table 2 are accurate to the specified uncertainties. The uncertainty in γ was found by finding the maximum and minimum amplitudes the

absorption plot could be fit by, and determining the corresponding γ for each amplitude. Then the difference between $\gamma_{maximum}$ and $\gamma_{minimum}$ was calculated and halved to give the γ of best fit uncertainty.

The uncertainty in ^{3}He density was calculated similarly. I shall call the uncertainty included in Equation 4 as K-D2 uncertainties and all other uncertainties, such as those cited in Table 2, as fitting uncertainties. If the K-D2 uncertainties are ignored in Equation 4, then the fitting uncertainties for ^{3}He density can be obtained quite easily. The maximum density achievable is found using Equation 4 with $\gamma_{maximum}$ and the minimum density achievable is found with $\gamma_{minimum}$. Then the maximum and minimum densities are subtracted and halved to determine the ^{3}He density uncertainty. The quoted ^{3}He density value in Table 2 is obtained using Equation 4 and the γ of best fit value.

The calculated ^{3}He densities in Table 2 for file names 2009_03_25_14_43, 2009_03_25_15_07, 2009_03_25_15_46, and 2009_04_01_13_49 have uncertainties that agree with the known ^{3}He density of the target cell. The remaining files have such low density measurements that they were omitted from the total average ^{3}He density for Fini. The total average ^{3}He density for Fini is 7.12 +/- 0.83 amg incorporating fitting errors only. This is consistent from the density estimated at the time the cell was produced. Curve-fit screenshots of each file name are given in Figures 20-26.

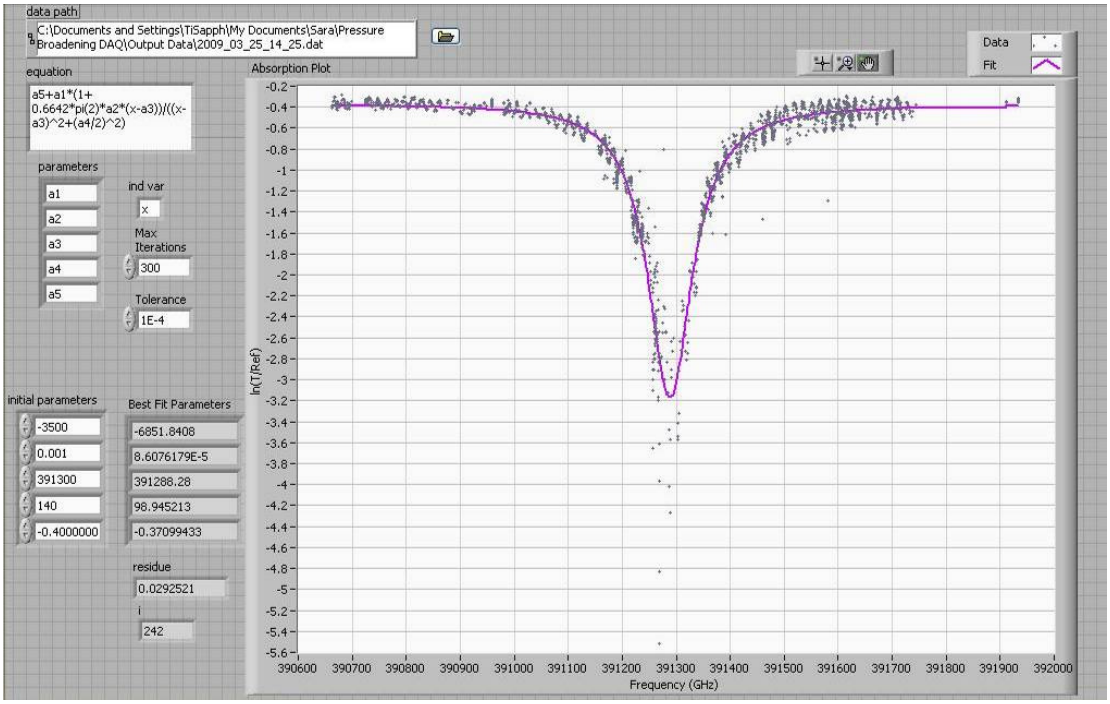

Figure 20: Curve fit of file name 2009_03_25_14_25 with 10mW of laser power into blue fiber.

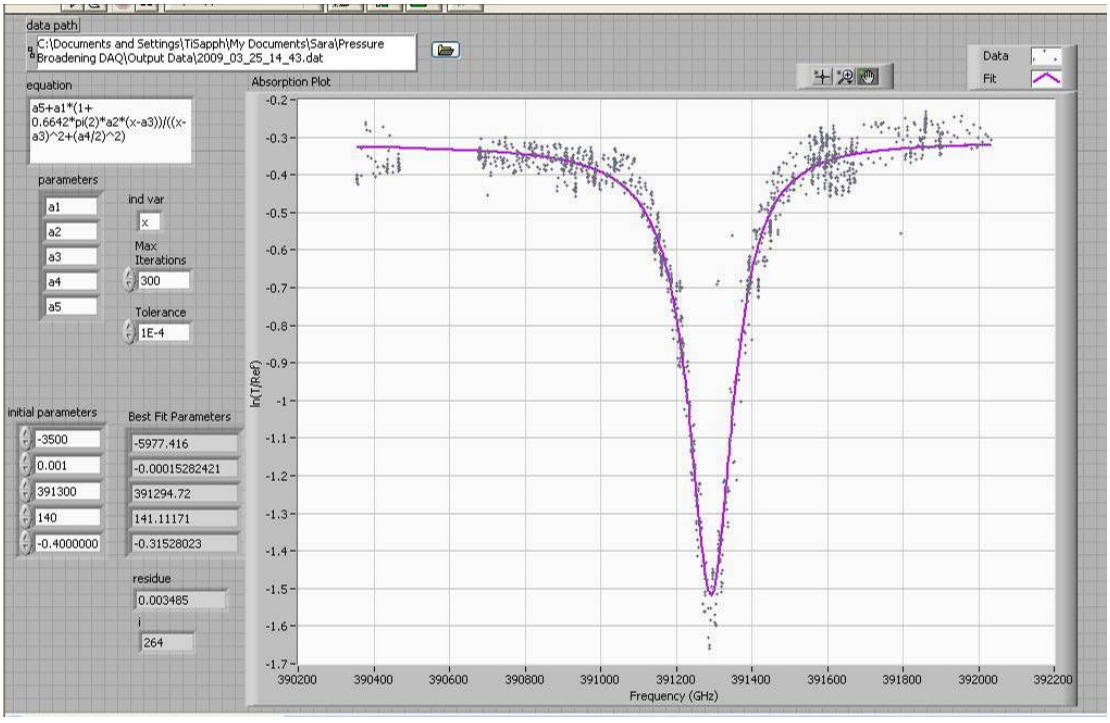

Figure 21: Curve fit of file name 2009_03_25_14_43 with 15mW of laser power into blue fiber.

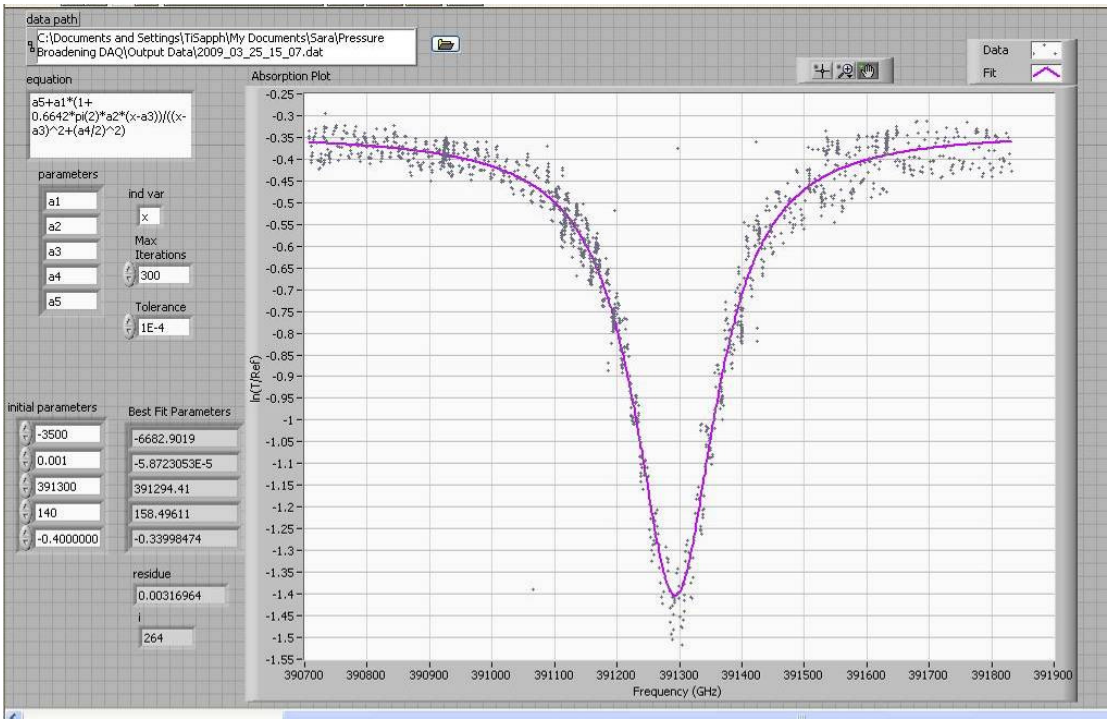

Figure 22: Curve fit of file name 2009_03_25_15_07 with 20mW of laser power into blue fiber.

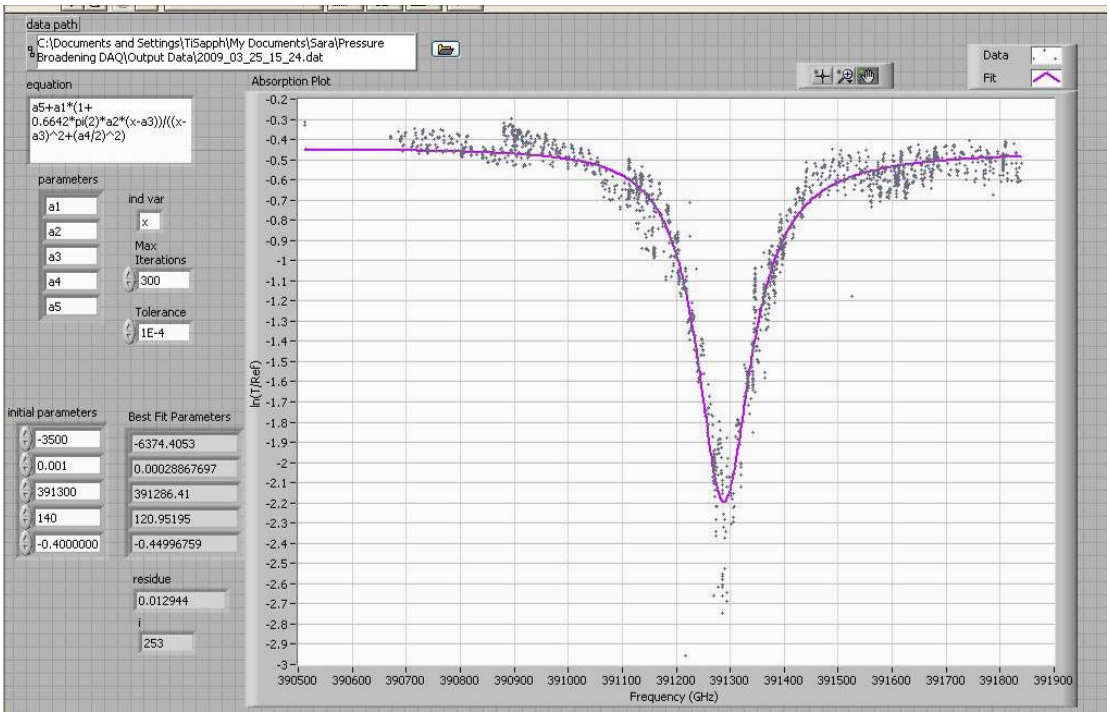

Figure 23: Curve fit of file name 2009_03_25_15_24 with 25mW of laser power into blue fiber.

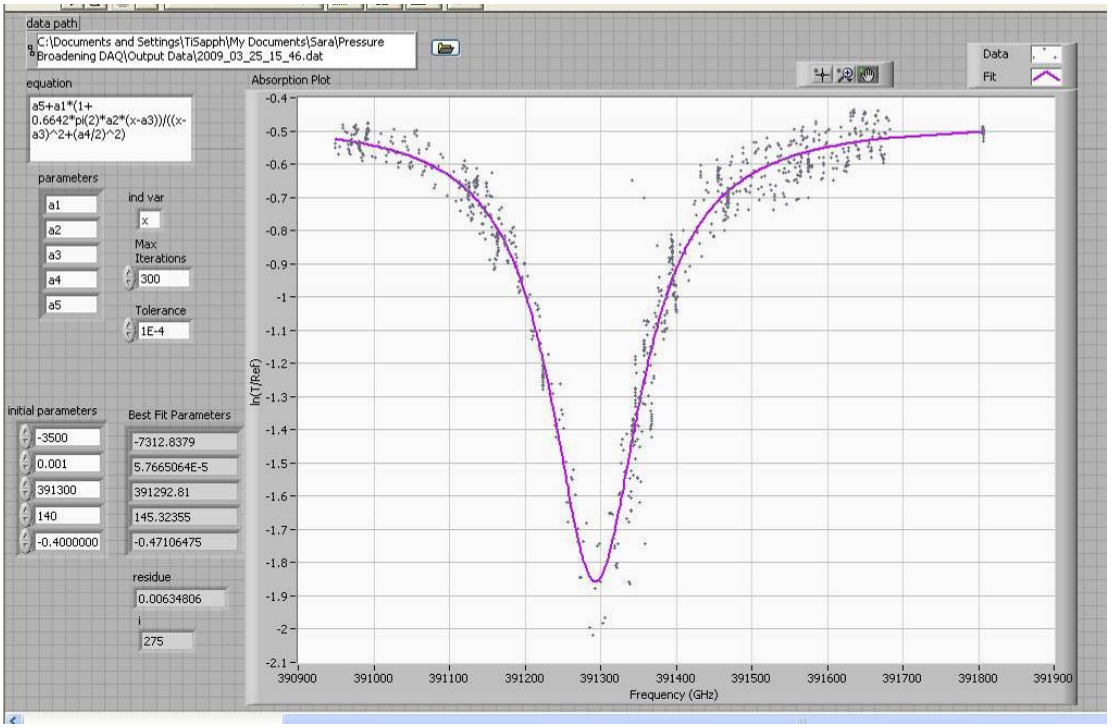

Figure 24: Curve fit of file name 2009_03_25_15_46 with 5mW of laser power into blue fiber.

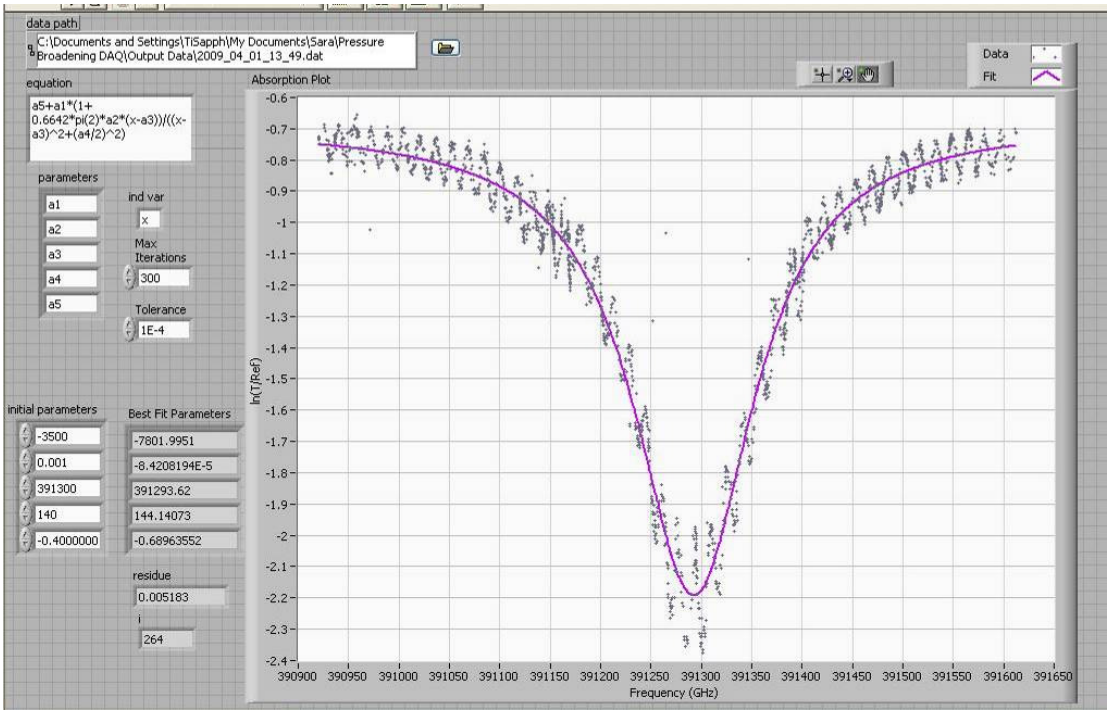

Figure 25: Curve fit of file name 2009_04_01_13_49 with 15mW of laser power into blue fiber.

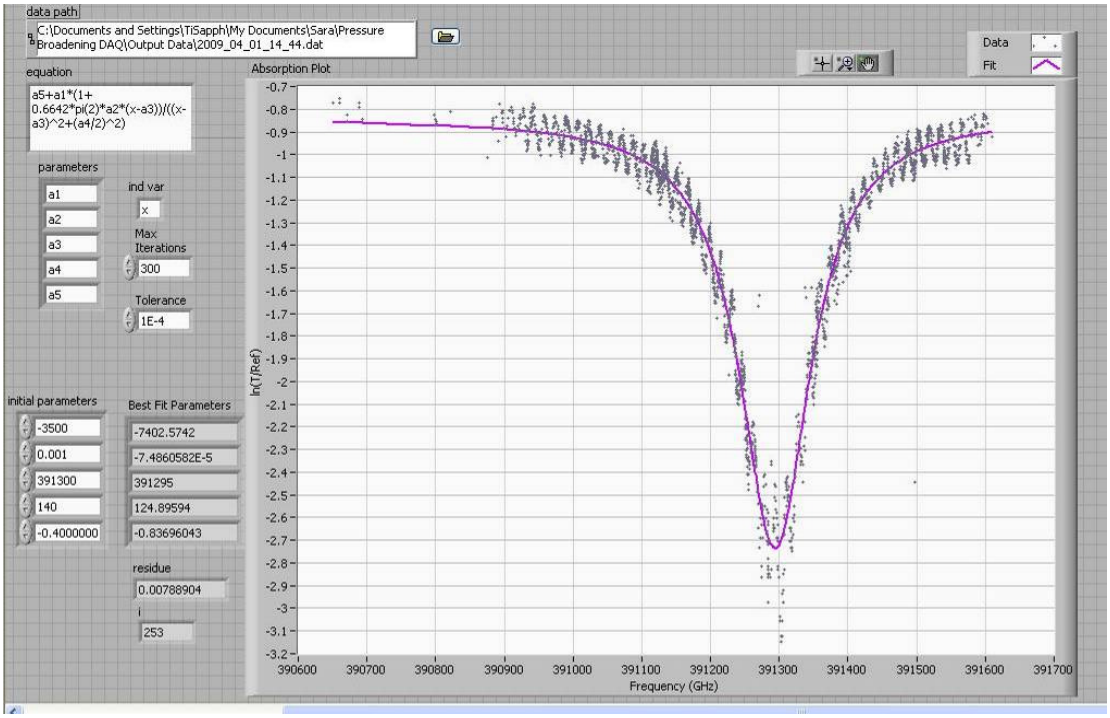

Figure 26: Curve fit of file name 2009_04_01_14_44 with 20mW of laser power into blue fiber.

The K-D2 uncertainties contribute additional uncertainty that must be accounted for. This additional uncertainty can be stated as a percent uncertainty due to the maximum and minimum values of the conversion function available for K D2 absorption in ^{3}He. The maximum value of the conversion function is 23.14 and the minimum value of the conversion function is 19.63. The K-D2 uncertainty in density due to the uncertainty in the conversion function is 16.4% (rel).

Figure 27 shows a plot of ^{3}He densities versus laser power input based on data from Equation 4. No correlation appears to be present between the two parameters.

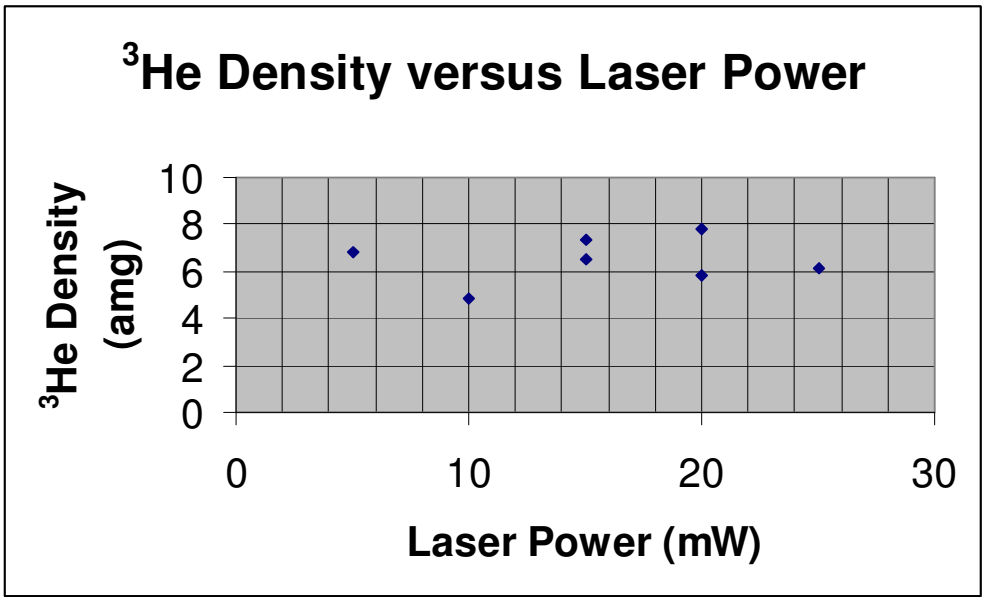

Figure 27: Plot showing no correlation between ^{3}He density and input laser power.

CONCLUSION

In conclusion, the density of ^{3}He gas can be measured with a laser that has an adjustable frequency. This process is called pressure broadening and is very useful when characterizing ^{3}He target cells for TJNAF.

The data shown seems reasonably well-behaved at 125°C but more research is needed at higher temperatures. Absorption scans at 130°C and 135°C would be helpful in knowing what, if any, upper threshold in temperature exists. It could be possible that the noise will decrease and that a larger absorption peak occurs.

While the data gathered thus far is certainly good data, it could be better. There is noticeable noise on all the absorption plots and the next step in this research will be to investigate how to diminish this noise. An optical chopper and lock-in amplifier might help to reduce any noise picked up by experimental equipment once the Ti:Sapph laser reaches the oven optical table.

Much can be done to improve the accuracy of the photodiode sensors as well. First, it would be helpful to place a focusing lens in front of each photodiode to centralize the laser beam onto the photodiode's sensor. Doing this should give a more accurate reading of the intensity of the laser light. Second, the photodiodes may be experiencing intensity nonlinearities when the laser frequency is tuned. If this is the case, then we can decrease the light. Thirdly, the intensity range of the photodiodes needs to be determined. Ideally the photodiodes should not have measurements near zero because of poor signal to noise ratio. If they do have these low measurements, then the laser intensity should be increased or the oven temperature reduced appropriately.

The pressure broadening code itself could be improved by specifying a certain number of measurements it should take at each wavelength within a particular scan. These measurements could be averaged together to give a mean measurement at each particular wavelength. This should produce more accurate data but might significantly increase the time to complete a scan.

In the future, we hope to improve the experiment by incorporating a mechanical arm to turn the coarse frequency tuner on the Ti:Sapph cavity. This would hopefully make scanning more time efficient and might produce cleaner looking data for curve-fitting.

Hopefully, the results of this research will aid William and Mary's endeavor to not only fill but also characterize the density of ^{3}He target cells.

REFERENCES

[1] M. McGuigan, Honors Thesis, *Measuring the Wall Thickness and Density of a ^{3}He Target Cell*, William and Mary, unpublished. Aug. 2002.

[2] J. P. Chen, Thomas Jefferson National Accelerator Facility, private communication, July 2007.

[3] J. Katich, Thomas Jefferson National Accelerator Facility, private communication, July 2007.

[4] P. Mastromarino, C. Otey, E. Hughes, *Density Project Summary*, unpublished, California Institute of Technology, 2001.

[5] K. J. Slifer, *Spin Structure of ^{3}He and the neutron at Low Q^2; A Measurement of the Extended GDH Integral and the Burkhardt-Cottingham Sum Rule*, Ph.D. dissertation, Temple Univ., Philadelphia, PA, 2004.

[6] M. V. Romalis, Doctoral Thesis, *Laser Polarized ^{3}He Target Used for a Measurement of the Neutron Spin Structure*, Princeton University, 1997.

[7] J. Singh, *On Hybrid Pressure Broadening Studies*, University of Virginia, 2006.

[8] J. Singh, University of Virginia, private communication, April 2009.

[9] T. Ban, D. Aumiler, R. Beuc, G. Pichler, *Rb_2 Diffuse Band Emission Excited by Diode Lasers*, The European Physical Journal D, Vol. 30, 2004.

[10] H. Haken, H. Wolf, W. Brewer, *The Physics of Atoms and Quanta*, Heidelberg, Berlin, 7th ed., 2005.

[11] Todd Averett, The College of William and Mary, private communication, April 2009.